J|A|C|S
COMMUNICATIONS

Published on Web 03/06/2003

Spatially and Temporally Resolved Delivery of Stimuli to Single Cells

Bingyun Sun and Daniel T. Chiu*

Department of Chemistry, University of Washington, Seattle, Washington 98195-1700

Received December 27, 2002 ; E-mail: chiu@chem.washington.edu

Cells respond to their environment through a complex and interdependent series of signal transduction pathways that frequently begin at the cell membrane with high spatial and temporal resolutions (e.g., exocytosis, endocytosis, synaptic transmission).[1] This plasma membrane defines the boundary of the cell, encloses the cytosol, and maintains the intracellular environment. The cell membrane not only acts as a barrier that protects the cell from the extracellular space but with its embedded receptors, surface-anchored proteins, and signaling molecules serves also as a sensor and communicator to the extracellular world.[1] Although a typical mammalian cell measures only 10−20 μm in diameter, the cell is a highly organized and spatially heterogeneous structure. To study and dissect the mechanism and signaling pathways by which a single cell processes the arrival of a particular signal at its membrane surface, we have developed a technique by which a precisely timed stimulus can be delivered to the cell with high spatial resolution.

To evoke a ligand-induced response from a cell, most experiments have relied on the perfusion of the cell in a microchamber[2] or with pressure microinjection,[3] on iontophoresis,[4] or on the flash photolysis of a caged compound.[5] Although the implementations of perfusion and iontophoresis are straightforward and their strategy is generally applicable, these approaches typically lack both high spatial and temporal resolution.[3a,4b] UV photolysis of a caged compound, in combination with two-photon excitation,[6] can overcome many of the spatial and temporal limitations of perfusion and iontophoresis. The spatial resolution of two-photon excitation is typically on the order of several hundred nanometers, defined mostly by the tightness of the laser focus.[6a,c] The temporal resolution of two-photon uncaging varies and is limited by the time scale of the photochemical steps by which the photolysis of the caging group occurs, which is typically in the tens of microseconds to milliseconds range.[7] Despite the good spatial and temporal resolution that can be achieved by using two-photon photolysis of a caged molecule, the use of a caged compound suffers from a number of drawbacks: (1) The design and synthesis of a suitable caged molecule are complex and time-consuming, (2) the caging of large bioactive molecules such as peptides (e.g., cytokines) and proteins is difficult if at all possible, and (3) the uncaging of multiple stimuli simultaneously is often cumbersome.

This Communication describes a new strategy for delivering defined packages of stimuli to single cells with both high spatial and temporal resolutions. Figure 1A schematically depicts our approach. Optical trapping is used to manipulate individual vesicles (or any suitable nanocontainers) that encapsulate the bioactive molecules of interest. Once a select vesicle is placed adjacent to the target cell, a single 3-ns pulse from a UV laser (337 nm), which is aligned collinear with the trapping laser (1064 nm), is used to photolyze the optically trapped vesicle and to release the encapsulated molecules. Pulsed UV laser can provide short wavelength light with high instantaneous power and is widely used in photoablating biotissues and polymers.[8] Figure 1B shows the positioning and trapping of a single 0.1 μm (in diameter) vesicle, which was formed by extrusion, in contact with a CHO-M1 cell.

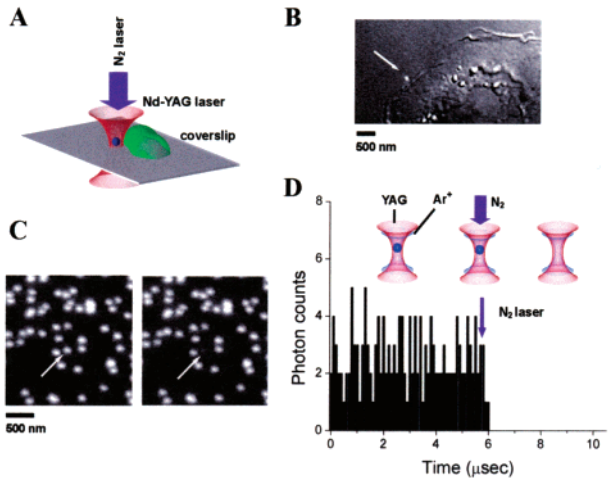

Figure 1. (A) Schematic illustration of the relative positions of the YAG laser (red; 1064 nm; ∼0.3 W prior to entering the N.A. 1.3 oil immersion objective), the trapped vesicle (blue), the target cell (green), and the N_2 laser (purple; 337 nm; ∼1 μJ prior to entering the objective). (B) Fluorescence−Normaski image showing the precise positioning of a single 0.1 μm DiO-C18 stained vesicle adjacent to a CHO-M1 cell. (C) Demonstration of the spatial resolution of the focused N_2 laser in which a single 0.11 μm fluorescent beads (arrow) was photolyzed by a single 3 ns N_2 laser pulse. (D) Demonstration of the temporal resolution of single-vesicle photolysis, in which the vesicle was photolyzed within 0.3 μs; the inset depicts schematically the sequence of steps.

Figure 1C demonstrates the selective photolysis of a single 0.11 μm fluorescent polystyrene bead that was in close proximity (less than 0.2 μm) to another 0.11 μm bead. In contrast to the use of caged compounds in which the photolysis volume and thus the spatial resolution is determined by the excitation focal volume, the photolysis volume in our approach is defined by the size of the vesicle and by the ability to optically trap and precisely position such small vesicles. In principle, by using small nanocontainers (e.g., less than 0.1 μm), the photolysis volume can be significantly smaller than the laser excitation volume defined by the tight focus. It is also possible to spectrally select the vesicle to be photolyzed by doping the vesicle membrane with absorptive dyes that are tuned to the photolysis wavelength.[9]

Figure 1D illustrates the time scale of photolyzing a single vesicle; the inset schematically illustrates the experiment. A single 1 μm vesicle, which was stained with a membrane dye (DiO-C18), was first optically trapped in solution. The fluorescence signal from the trapped vesicle was continuously monitored with a confocal detection system in which the laser focus of the Ar^+ laser (488 nm) was aligned collinear with the trapping laser. At 5.0 μs, a trigger was sent from the computer to initiate the firing of a single 3 ns pulse from the N_2 laser, which was aligned collinear with both the trapping laser and Ar^+ laser. The arrival of the N_2 laser pulse onto the trapped vesicle (arrow), which was measured to occur at 0.7

10.1021/ja029942p CCC: $25.00

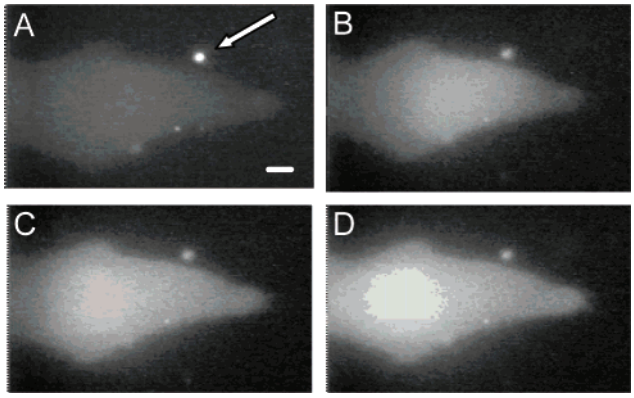

Figure 2. Response of a fluo-3 loaded CHO-M1 cell to carbachol, which was released from the photolysis of a single 0.6 μm vesicle. (A) Image of the vesicle and the cell before vesicle (arrow) photolysis. (B)−(D) Sequential fluorescent images showing the increase of the intracellular calcium level after vesicle photolysis. The time interval between A and B is 1 s, while the time intervals from B to C and from C to D are 0.15 s, and 0.55 s, respectively. The vesicle was formed in HEPES buffer (pH 7.4) containing 0.1 M carbachol and was doped with cholesteryl 1-pyrenebutyrate and DiO-C18 at 50 and 1 mol %, respectively. The scale bar represents 1 μm.

μs after triggering, caused the photolysis of the vesicle and the disappearance of the fluorescence signal. Photolysis of a single vesicle occurs within 0.3 μs, which is significantly shorter than the uncaging times of most caged molecules.

To demonstrate the applicability of this approach for the spatially resolved delivery of stimuli to single cells, we encapsulated carbachol into the vesicle interior. Carbachol binds to the muscarinic acetylcholine receptors[10] and activates G-protein that hydrolyzes phosphoinositide to produce IP_3, which then causes the increase of the intracellular levels of calcium.[11] We visualized this increase with the fluorescent calcium indicator, fluo-3. Figure 2 shows the activation of a fluo-3 loaded CHO-M1 cell that has been transfected to express muscarinic acetylcholine receptors (CHO-M1-WT3, ATCC). A single 0.6 μm vesicle was positioned with optical trapping at ~0.5 μm from the CHO-M1 cell. To visualize the small vesicle, we stained the vesicle membrane with 1% DiO-C18. The photolysis of the vesicle resulted in the release of the intra-vesicular carbachol and the collapse of the residual vesicle membrane onto the surface of the coverslip. The released carbachol caused the localized increase of intracellular calcium, which propagated throughout the entire cell (Figures 2B−2D). The amount of stimuli to be delivered to the cell can be varied easily by controlling either the size of the vesicle or the concentration of the stimuli during their encapsulation into the vesicle.[12] In contrast to the use of caged compounds, all biologically active molecules are confined to the vesicular interior, thus avoiding any undesirable side effects that may be caused by the presence of caged or partially uncaged molecules in contact with cells.[13] Therefore, our technique is based on the physical separation of the stimuli from cells, rather than relying on "chemical" separation as is the case for caged compounds.

The main drawback of our approach lies in the finite size of the vesicles, which may make them unsuitable for intracellular applications. Although methods exist for introducing small nanoparticles into single cells,[14] the intracellular diffusion of these nanoparticles may be restricted. For the introduction of extracellular stimuli, however, this method possesses a number of advantages: (1) Any membrane impermeable molecules, including peptides and proteins, can be encapsulated into vesicles (or other nanocontainers) and be delivered to cells, (2) it is straightforward to deliver multiple stimuli, with each stimulus present at a given concentration, to single cells simultaneously, (3) all stimuli are confined to the vesicle interior and are physically and spatially separated from the cells, and (4) it is possible to spectrally tuned the photolysis wavelength by doping the vesicle membrane with the appropriate absorptive dyes. The strategy we described is not limited to vesicles but to any nanocontainers of choice. For quantitative applications in which the amount of stimuli delivered must be controlled, the size of the extruded vesicle must be uniform, which can be achieved by purifying the vesicles with respect to size using methods of separation. Alternatively, monodispersed non-vesicle based nanocontainers may be designed and synthesized. This technique offers new possibilities in the study of the heterogeneous organization of single cells and the probing of the dynamics of cellular responses after a precisely timed delivery of stimuli.

Acknowledgment. B. Sun acknowledges support from the Center for Nanotechnology at the University of Washington for an UIF fellowship. This work was partially supported by NIH (GM 65293, DA 16249) and by starter grants from Research Corporation (RI 0631) and the Dreyfus Foundation (NF-00-077).

Supporting Information Available: A movie of Figure 2. This material is available free of charge via the Internet at http://pubs.acs.org.

References

(1) Jahn, R.; Südhof, T. C. *Annu. Rev. Biochem.* **1999**, *68*, 863−911.
(2) (a) Spitzer, K. W.; Bridge, J. H. B. *Am. J. Physiol.* **1986**, *256*, C441−C447. (b) Pelc, R.; Ashley, C. C. *Eur. J. Physiol.* **1997**, *435*, 174−177.
(3) (a) Angelantonio, S. D.; Nistri, A. *J. Neurosci. Methods* **2001**, *110*, 155−161. (b) Akaoka, H.; Saunier, C. F.; Chergui, K.; Charlety, P.; Buda, M.; Chouvet, G. *J. Neurosci. Methods* **1992**, *42*, 119−128.
(4) (a) Junginger, H. E. *Adv. Drug Delivery Rev.* **2002**, *54*, S57−S75. (b) Awenowicz, P. W.; Porter, L. L. *J. Neurophysiol.* **2002**, *88*, 3439−3451.
(5) (a) Adams, S. R.; Tsien, R. Y. *Annu. Rev. Physiol.* **1993**, *55*, 755−784. (b) Gurney, A. M.; Lester, H. A. *Physiol. Rev.* **1987**, *67*, 583−617. (c) Hess, G. P. *Arch. Physiol. Biochem.* **1996**, *35*, 752−761. (d) Hess, G. P.; Grewer, C. *Methods Enzymol.* **1998**, *291*, 443−473.
(6) (a) Denk, W.; Strickler, J. H.; Webb, W. W. *Science* **1990**, *248*, 73−76. (b) Albota, M.; Beljonne, D.; Brédas, J.-L.; Ehrlich, J. E.; Fu, J.-Y.; Heikal, A. A.; Hess, S. E.; Kogej, T.; Levin, M. D.; Marder, S. R.; McCord-Maughon, D.; Perry, J. W.; Röckel, H.; Rumi, M.; Subramaniam, G.; Webb, W. W.; Wu, X.-L.; Xu, C. *Science* **1998**, *281*, 1653−1656. (c) Shear, J. B. *Anal. Chem.* **1999**, 71, 569A−642A.
(7) (a) Brown, E. B.; Shear, J. B.; Adams, S. R.; Tsien, R. Y.; Webb, W. W. *Biophys. J.* **1999**, 76, 489−499. (b) Lempert, W. R.; Harris, S. R. *Meas. Sci. Technol.* **2000**, *11*, 1251−1258.
(8) Srinivasan, R. *Science* **1986**, *234*, 559−565.
(9) Bisby, R. H.; Mead, C.; Morgan, C. G. *FEBS Lett.* **1999**, *463*, 165−168.
(10) Jones, S. V.; Choi, O. H.; Beaven, M. A. *FEBS Lett.* **1991**, *289*, 47−50.
(11) Berridge, M. J.; Lipp, P.; Bootman, M. D. *Nature Rev. Mol. Cell. Biol.* **2000**, *1*, 11−21.
(12) Walde, P.; Ichikawa, S. *Biomol. Eng.* **2001**, *18*, 143−177.
(13) Walker, J. W.; McCray, J. A.; Hess, G. P. *Biochemistry* **1986**, *25*, 1799−1805.
(14) (a) Karlsson, M.; Nolkrantz, K.; Davidson, M. J.; Strömberg, A.; Ryttsén, F.; Åkerman, B.; Orwar, O. *Anal. Chem.* **2000**, *72*, 5857−5862. (b) Dubertret, B.; Skourides, P.; Norris, D. J.; Noireaux, V.; Brivanlou, A. H.; Libchaber, A. *Science* 2002, *298*, 1759−1762.

JA029942P